Int. J. Heat Mass Transfer. Vol. 37, No. 1, pp. 53–67, 1994
Printed in Great Britain

0017–9310/94 $6.00+0.00

Enhancement of CHF water subcooled flow boiling in tubes using helically coiled wires

G. P. CELATA, M. CUMO and A. MARIANI
ENEA C.R.E. Casaccia, Via Anguillarese, 301, 00060 Rome, Italy

(*Received 2 March 1993 and in final form 22 June 1993*)

Abstract—The present paper reports the results of an experimental investigation about the occurrence of the critical heat flux (CHF) in subcooled flow boiling of water, carried out to ascertain the influence of thermal hydraulic parameters on CHF under conditions typical of thermonuclear fusion divertor thermal hydraulic design. Helically coiled wires were used as turbulence promoters to enhance the CHF with respect to the smooth channel. Geometric characteristics of stainless steel 304 Type test sections were: 6.0 and 8.0 mm i.d., 0.25 mm wall thickness, 0.1 and 0.15 m heated length, horizontal and vertical (upflow) position. Test sections were uniformly heated using d.c. current. A maximum CHF of about 30 MW m^{-2} was reached with smooth tubes under the following conditions: $T_{in} = 30$°C, $p = 4.6$ MPa, $u = 10$ m s^{-1}, $D = 8.0$ mm, $L = 0.1$ m. Helically coiled wires ($d = 1.0$ mm, pitch $= 20.0$ mm) allowed an increase of the CHF up to 50%, with reference to smooth channels, coupled with a moderate increase of pressure drop (down to 25%). Pressure revealed a negative effect on the efficiency of turbulence promoters. No observable influence of the channel orientation was detected.

INTRODUCTION

AT THE present time fusion technology raises some of the most formidable engineering problems ever encountered. One of them is related to the thermal hydraulics and particularly to the heat removal from components such as divertors, plasma limiters, neutral beam calorimeters, ion dump and first-wall armor that are estimated to be subjected to very high heat loads. The order of magnitude of heat fluxes to be removed ranges from 2 to 60 MW m^{-2}, i.e. at least an order of magnitude higher than in an LWR situation. Thus, the available experimental data, essentially obtained in LWRs conditions, are consequently not consistent with the present problem, and existing theories are often bound to fail in describing the phenomenological behaviour. Among possible techniques for the removal of these high heat fluxes, subcooled flow boiling turns out to be the more attractive, from an engineering viewpoint, as it can accommodate very high heat transfer rates. Subcooled flow boiling has been widely investigated in the past [1–3]. As it is well known, this forced convective boiling involves a locally boiling liquid, whose bulk temperature is below the saturation, flowing over a surface exposed to a high heat flux, and is one of the most efficient techniques of removing high heat fluxes. However, successful use of subcooled flow boiling for high heat fluxes removal requires the critical heat flux (CHF), which is described as a sharp reduction in the energy transfer from a heated surface, not to be reached. The occurrence of CHF, for the case of heat flux controlled systems, results in a significant increase in the wall temperature that is usually well above that at which serious damage or 'burnout' of the heating surface occurs. In 1984 Boyd [4, 5] reported a thorough review of CHF in subcooled flow boiling (with about 300 papers quoted), confirming that studies performed so far are mainly devoted to the thermal hydraulics of LWRs (heat fluxes around 1 MW m^{-2}). Fusion technology requirements gave rise in recent years to a rush in the production of experimental data and theoretical models for subcooled flow boiling CHF. A brief review of experimental data and models recently published is given by Celata [6]. The main aim of the present research was to provide basic information on CHF in water subcooled flow boiling in 6.0 and 8.0 mm i.d. tubes, with and without turbulence promoters (helically coiled wires). These latter are used to enhance the CHF with regard to the case of the smooth tube.

EXPERIMENTAL APPARATUS AND TEST SECTIONS

The schematic diagram of the employed water loop is drawn in Fig. 1. The loop is made of Type 304 stainless steel and filled with tap water passed through deionizing particulate beds (not shown in the figure). The alternative pump (a three-head piston pump), the maximum volumetric flow rate of which is 2000 l h^{-1}, is connected to a damper to further reduce pressure oscillations while maintaining stable flow conditions (residual pulsation 2.5%). A turbine flow meter is installed to measure the water flow rate. The test section is generally vertically oriented with water flowing upwards. Test sections (one for each run) are made of Type 304 stainless steel (electric resistivity at 500 K is 93 $\mu\Omega$ cm), 0.25 mm in wall thickness, uniformly heated over a length of 0.1 m by Joule effect using a

NOMENCLATURE

Bo	boiling number, $q''/G\lambda$
C	parameter defined in (7) and (10)
CHF	critical heat flux [W m^{-2}]
C_p	specific heat [J kg^{-1} K^{-1}]
D	channel diameter [m]
d	wire diameter [mm]
F	parameter defined in (6)
FM	figure of merit, defined in (4)
G	mass flux [kg m^{-2} s^{-1}]
h	enthalpy [J kg^{-1}]
h_t	heat transfer coefficient [W m^{-2} K^{-1}]
K	thermal conductivity [W m^{-1} K^{-1}]
k	velocity coefficient
L	channel length [cm]
L_a	entrance length [cm]
L_B	vapour blanket length [μm]
p	pressure [MPa]
Pr	Prandtl number, $C_p\mu/K$
q''	heat flux [W m^{-2}]
R	ideal gas constant on a unit mass basis
Re	Reynolds number, GD/μ
t	wall thickness [mm]
T, ΔT	temperature, temperature difference [°C, K]
u	velocity [m s^{-1}]
U_B	vapour blanket velocity [m s^{-1}]
U_δ	liquid sublayer velocity at δ [m s^{-1}]
x	thermal equilibrium quality.

Greek symbols

γ	wire pitch [mm]
δ	liquid sublayer thickness [μm]
λ	latent heat [J kg^{-1}]
μ	dynamic viscosity [kg m^{-1} s^{-1}]
ρ	density [kg m^{-3}]
σ	surface tension [N m^{-1}]
Ψ	parameter defined in (10).

Subscripts

CHF	pertains to burnout conditions
conv	convective
cr	critical (thermodynamic) conditions
ex	exit
f	pertains to the liquid in saturated conditions
g	pertains to the vapour
in	inlet
l	pertains to the liquid
max	maximum
out	outlet
pb	pool boiling
sat	saturated conditions
sub	subcooled conditions
w	pertains to the wall.

200 kW (50 V and 4000 A, d.c.) electric feeder. Of course not all the electrical power is available for the test section, as it depends on the electrical resistance of this latter, which is a function of the diameter and of the temperature (through the electrical resistivity). Two different test section inner diameters were used: 6.0 and 8.0 mm$\pm$0.01 mm. In addition to the heated length of 0.1 m, for the test section $D = 8.0$ mm, some tests were carried out with a heated length of 0.15 m, and, among these, some were performed with the test section placed in the horizontal position. For the $D = 8.0$ mm, $L = 0.1$ m test section, tests were carried out with the insertion of helically coiled wires inside the tube as turbulence promoters (characteristics of wires will be given in the Experimental Results Sections). Wires are of spring steel, and their presence does not appreciably affect the electrical resistance of the tube. The test section is connected to copper feed clamps, by means of which it is possible to transfer the electric current to the tube. The power was computed by evaluating the product of the voltage drop across the test section and the current flowing through the walls of the test section. The current was computed from the measurement of the voltage drop (in millivolts) across a precision shunt resistor. Thermal expansion of the test section is mechanically allowed ($\sim$1.5 mm), thus preventing the rupture of the tube due to thermally induced compressive stresses. Before entering the test section, the water flows through an unheated tube, of the same diameter as the test section, to assure that the liquid velocity profile is fully developed. The un-heated tube length is twice the entrance length, L_a, calculated, under the most severe conditions (highest value of Reynolds number), using [7]:

$$\frac{L_a}{D} = 0.008\,Re^{0.685}. \qquad (1)$$

Pressure taps are placed just upstream of the unheated length inlet and just downstream of the heated length exit. The static pressure is measured by unsealed strain-gauge absolute pressure transducers. It is therefore possible to evaluate the pressure gradient in the test channel once the hydraulic characteristics under no-power conditions are known. The pressure at the exit of the test channel is regulated by an electrically controlled valve. The bulk fluid temperature is measured just upstream, $T_{f,in}$, and downstream, $T_{f,out}$, this latter, after a suitable mixing of the liquid, of the test section using 0.5 mm K-type thermocouples. The knowledge of $T_{f,in}$ and $T_{f,out}$,

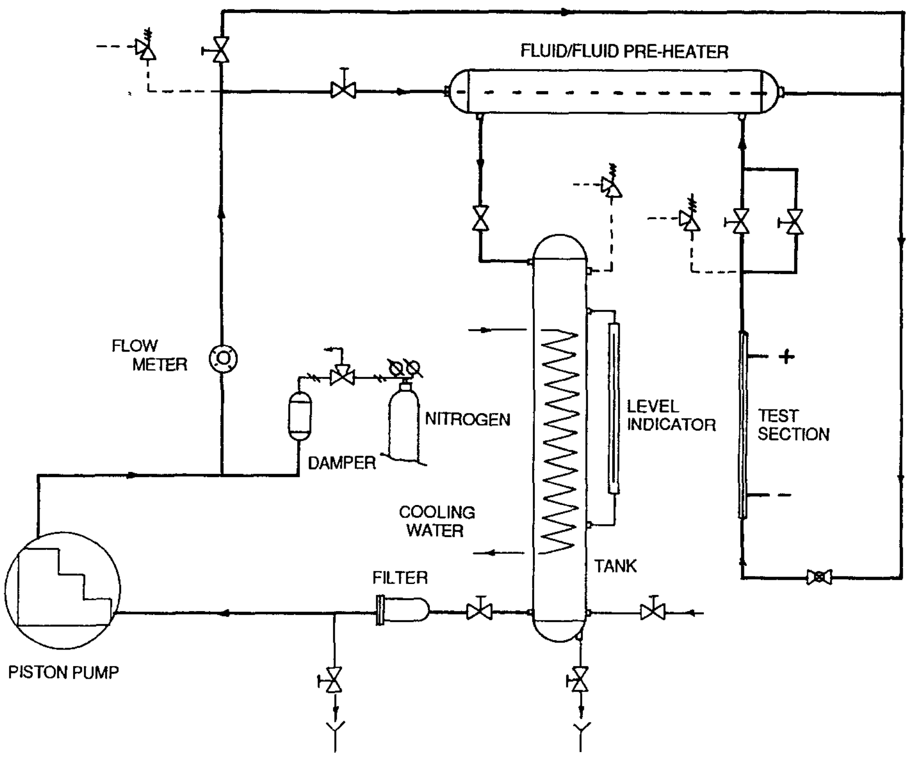

FIG. 1. Schematic of the experimental loop.

together with the measurement of the water mass flow rate, allows the computation of the thermal power delivered to the fluid by the heat balance in the coolant (calorimetric method). In fact, in all the tests performed (even at burnout conditions), the outlet bulk fluid temperature measurements always revealed the subcooling conditions of the water bulk at the test section exit. In this way the heat loss computation from the test section is bypassed. The employed test sections are not instrumented with wall thermocouples.

Downstream of the test section, the fluid passes

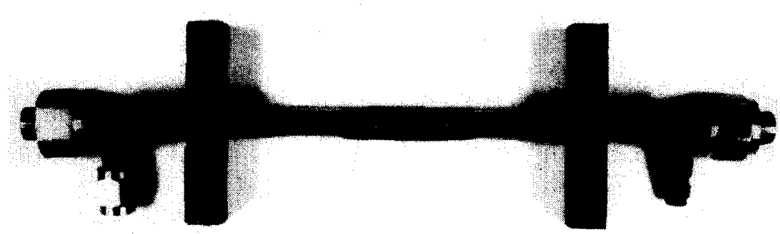

FIG. 2. Picture showing a split of the test section with the wire inserted.

through the fluid-to-fluid pre-heater and then in the water cooled tank, where the fluid is cooled down to 25°C even at the maximum thermal power delivered to the fluid, closing the loop through the filter, towards the piston pump. The maximum pressure of the loop is 7.0 MPa, while the maximum operating temperature of the pump is 70°C. The fluid-to-fluid pre-heater allows us to carry out experiments with a water inlet temperature above 70°C. Figure 2 shows a split of a test section with the wire inserted.

EXPERIMENTAL PROCEDURE

All the parameters are continuously monitored using digital and analog displays, and each variation is recorded. The experimental procedure consists of the following actions. First, the mass flow rate is set up using the manual control of the piston pump. Second, the exit pressure is established using the exit control valve. Once flow rate and exit pressure are steady, thermal power is added to the test section. The control parameter used while approaching the CHF is the electrical power delivered to the walls of the test section, and the initial increment in thermal power is 0.5 kW. Once 70% of the expected CHF value, obtained using the Gunther correlation [8] which is very simple and gives a conservative prediction (u: m s^{-1}; ΔT_{sub}: K; q''_{CHF}: W m^{-2})

$$q''_{CHF} = 71\,987 u^{0.5} \Delta T_{sub}, \tag{2}$$

is reached, the increment is reduced to 0.1 kW (0.1–0.6% of the CHF). After each increment, small adjustments are made in both the exit pressure and flow rate, so that the exit flow conditions correspond to the desired ones. The above reported procedure is repeated until burnout occurs, evidenced by test section destruction and detected by the sharp drop in the electrical power. Video movies show the existence, at burnout, of a narrow glowing area uniformly distributed around the perimeter, and located within 5.0 mm from the top copper feed clamp. A computerized data acquisition system records the measured parameters at the occurring of burnout.

EXPERIMENTAL RESULTS

The main aim of this research, carried out under a precise NET (Next European Torus) requirement, was to characterize the CHF in subcooled flow boiling of water in smooth pipes and to ascertain the effect of helically coiled wires as turbulence promoters for the enhancement of the CHF. Experiments were carried out in tubes of 6.0 and 8.0 mm i.d. under thermal hydraulic conditions typical of the present NET diverter design. Further tests were performed outside the above range of interest because of the basic aims of the research. Effects of heated length and channel orientation (horizontal against vertical) were also investigated, together with the effect of tube diameter (6.0 and 8.0 mm). Test conditions were selected by the combination of the following parameters, for a total of 91 data points:

- tube inside diameter, D:
  - 6.0 and 8.0 mm ($\pm$0.01 mm)
- heated length, L:
  - 0.1 and 0.15 m
- wall thickness, t:
  - 0.25 mm ($\pm$0.01 mm)
- tube material:
  - AISI 304 Type
- water mass flux, G:
  - from 2 to 10 Mg m^{-2} s^{-1}
- exit pressure, p:
  - from 0.8 to 5.0 MPa
- water inlet temperature, T_{in}:
  - from 30 to 75°C
- (water inlet subcooling, $\Delta T_{sub,in}$:
  - from 95 to 230 K)
- orientation of the test section:
  - vertical and horizontal (only for L = 0.15 m)
- wire diameter, d:
  - 0.5, 0.7 and 1.0 mm
- wire pitch, γ:
  - from 1.5 to 20.0 mm
- wire material:
  - spring steel.

Tests with turbulence promoters were carried out only with the D = 8.0 mm test sections, L = 0.1 m, vertical position.

Smooth tube tests, D = 6.0 and 8.0 mm

Experimental results for CHF for D = 8.0 mm and L = 0.1 m (vertical position) are reported in Figs. 3–5, where the values of the parameters reported on the figures are the nominal ones. Figure 3 shows the CHF vs the mass flux G, for different water inlet temperature and exit pressures for all the D = 8.0 mm tests. It can be noticed that, within the investigated range of G, the CHF is almost an increasing linear function of the mass flux, other conditions being equal. The CHF increases up to a factor of about three passing from 2 to 10 Mg m^{-2} s^{-1} (p = 0.8 MPa and T_{in} = 30°C) and the slope of CHF vs G is almost independent of subcooling in the same range. It is obvious that, apart from the problem of the increasing pressure drop, higher values of the CHF could be obtained by further increasing the mass flux. A significant effect on the CHF is exerted by the water inlet temperature, i.e. the inlet subcooling, of course in the sense that at a lower inlet temperature (higher subcooling) a higher CHF is obtained. From the above figure, because of the strong influence of subcooling, is it not possible to tell apart the pressure and inlet subcooling effects on CHF. In fact, since tests were carried out at different pressures with constant inlet temperature (that means different inlet subcooling), besides the (possible) direct influence of the pressure, there is also a strong indirect effect due to the variation of the subcooling. The separate effect of

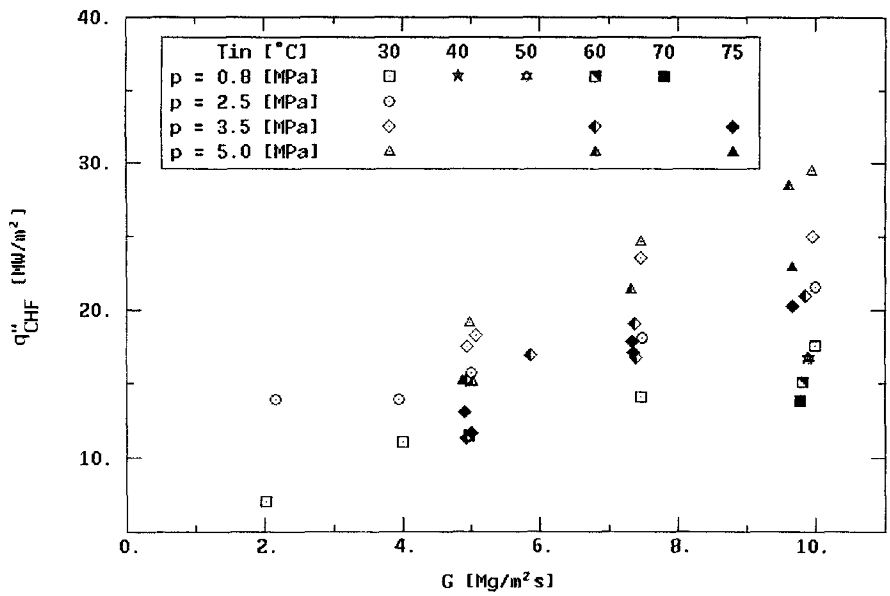

FIG. 3. CHF vs mass flux for all the $D = 8.0$ mm tests.

single parameters will be shown and analyzed in the next figures.

Figure 4 shows CHF vs water inlet subcooling for a fixed water velocity (10 m s^{-1}) and different pressures. CHF data as a function of $\Delta T_{sub,in}$ practically lie on a unique curve independent of the pressure. The fact that data grouped for different pressures at constant liquid velocity lie on a unique line when plotted as CHF vs $\Delta T_{sub,in}$, would suggest a negligible effect of the pressure on the CHF, at least in the range 0.8–5.0 MPa. The slight influence of the pressure on the CHF was already verified also by different authors in other experiments [6]. Finally in Fig. 5, CHF is plotted vs $\Delta T_{sub,in}$ for a fixed pressure ($p = 3.5$ MPa) and different velocities. Apart from some scattered data, the dependence of CHF on the inlet subcooling is almost linear. Therefore, acknowledging the slight direct influence of the pressure, this latter is anyway important in the sense that higher pressures, other conditions being equal, enable one to obtain higher liquid

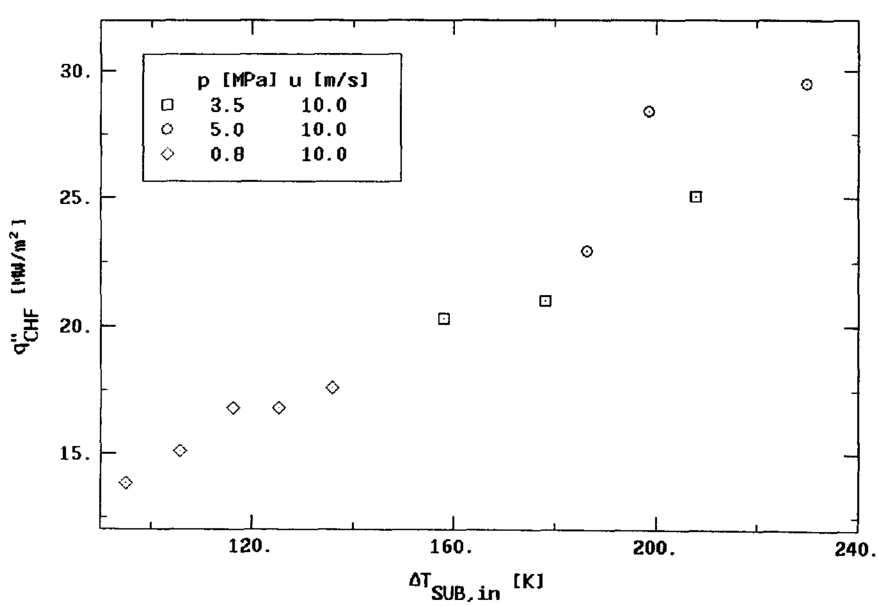

FIG. 4. CHF vs water inlet subcooling for a fixed water velocity ($u = 10.0$ m s^{-1}) and different pressure ($D = 8.0$ mm).

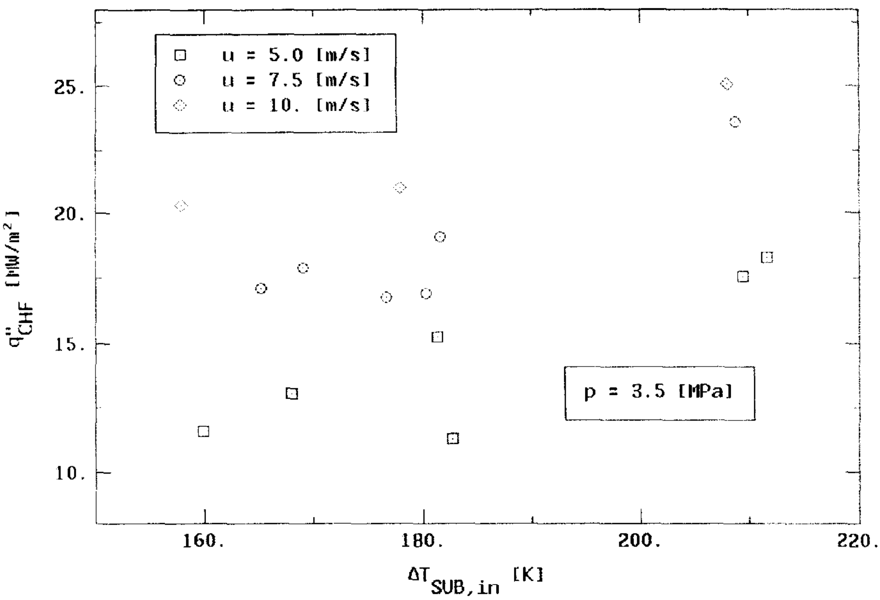

FIG. 5. CHF vs water inlet subcooling for a fixed exit pressure ($p = 3.5$ MPa) and different water velocity ($D = 8.0$ mm).

subcoolings, and, indirectly, contribute to the enhancement of the CHF. From Fig. 5 it is more evident that, at least in the present range, no inter-relation between G and $\Delta T_{sub,in}$ exists, as observed in Fig. 3. The same conclusion already drawn for the 8.0 mm data can be derived for the 6.0 mm data ($L = 0.1$ m, vertical position) that provide a confirmation of the already observed trends.

A direct comparison between 6.0 and 8.0 mm data is shown in Figs. 6 and 7. Figure 6 shows the CHF vs mass flux at 3.5 MPa and data-points are grouped according to inlet conditions. This is a pure engineering representation as, in the frame of the studies performed for NET design purposes, it was interesting to see the influence of the channel diameter for fixed inlet conditions. From the data plotted in Fig. 6, at least within the experimental uncertainty, no systematic evidence of the diameter effect can be observed. This means that the possible negative effect of the channel diameter on the CHF (as reported

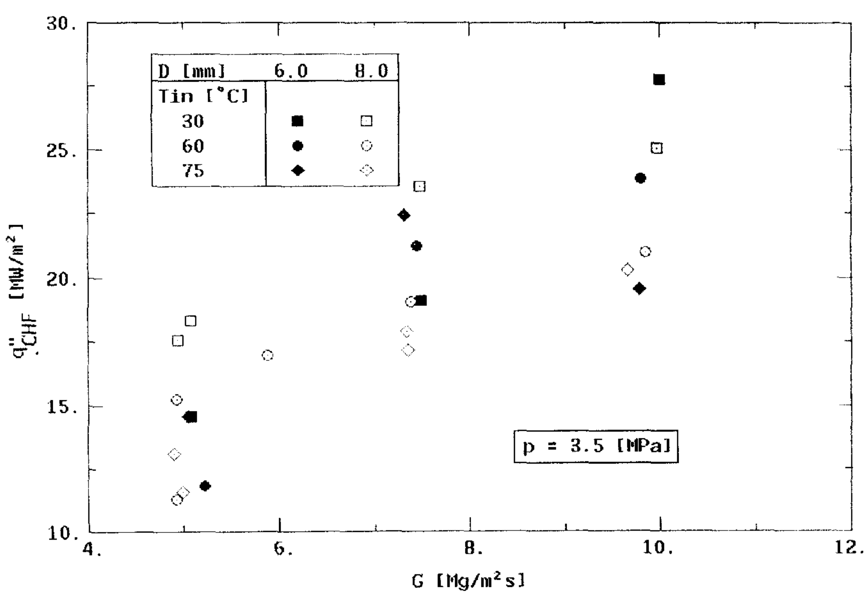

FIG. 6. Comparison between 6.0 and 8.0 mm CHF data at inlet conditions.

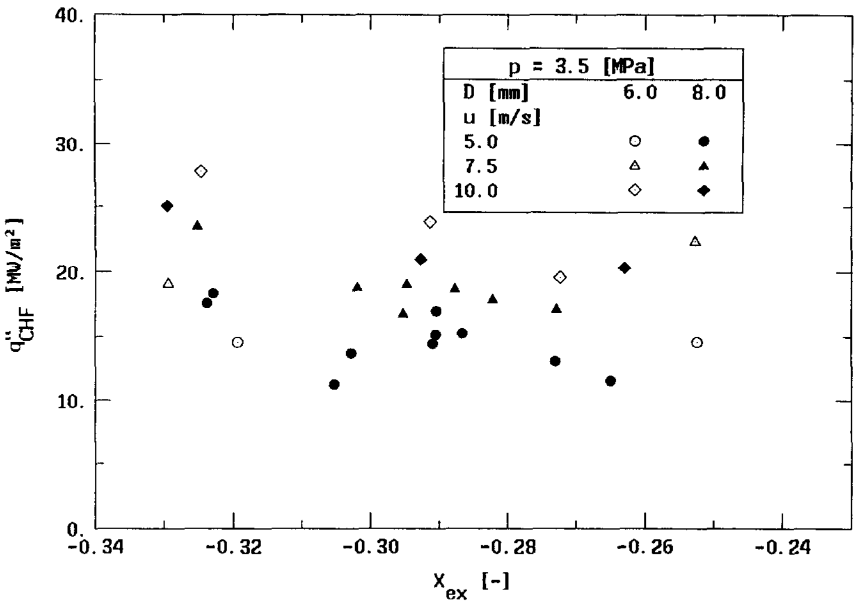

FIG. 7. Comparison between 6.0 and 8.0 mm CHF data at local conditions.

in the literature) is almost counterbalanced in the investigated range by the positive effect of more favourable exit thermal hydraulic conditions (subcooling) of the 8.0 mm data, due to the difference in the mass flow rate (thermal capacity). Figure 7 reports the CHF vs the calculated exit equilibrium quality x_{ex}, for the two different diameters and for different liquid velocities. This kind of presentation is based on a more scientific approach, that connects the CHF to local conditions, according to the school of thought considering burnout in subcooled flow boiling a local phenomenon, not strongly depending on the history of the thermal hydraulic conditions. From the plot of Fig. 7 it can be observed that under equal local thermal hydraulic conditions the effect of the diameter (between 6.0 and 8.0 mm) is practically negligible if coupled with not very high velocity. In practice, only at 10.0 m s^{-1} is it possible to ascertain from the graph a slightly higher CHF for the 6.0 mm than for the 8.0 mm data. Data carried out at 5.0 and 7.5 m s^{-1} show no difference between the two diameters. This conclusion is in good agreement with recent conclusions drawn in ref. [9]: increase of CHF with the decrease of tube inside diameter tends to be greater when associated with higher values of liquid velocity. Besides, the effect of the diameter on the CHF tends to weaken in the range of diameters of the present investigation.

From the analysis of experimental data shown in the previous figures we can notice that the maximum value of the CHF attainable in the investigated range is about 30 MW m^{-2} ($u = 10.0$ m s^{-1}; $D =$ 8.0 mm; $L = 0.1$ m; $p > 4.6$ MPa; $T_{in} = 30$°C and $\Delta T_{sub,ex} = 192$ K).

Another point of relevant interest may be the influence of the channel orientation and of the channel length on the CHF. Some tests were carried out with the purpose to ascertain this influence and the results are presented in Fig. 8, where CHF is plotted vs mass flux. In the range of liquid velocity of interest (2–8 m s^{-1}) horizontal against vertical data do not show any appreciable difference, while an increase of 50% of the heated length in the vertical position does not affect the CHF. The first observation, i.e. the independence of the CHF from the orientation of the channel, is of interest for practical purpose of NET, as the divertor is supposed to be inclined at about 30° from the horizontal and most research is conducted either with vertical or horizontal test sections.

Helically coiled wire tests

The limit of 30 MW m^{-2} is still too low a value if compared with what is requested by fusion reactor thermal hydraulics designers. On the other hand it is interesting to observe that according to Gambill and Lienhard [10] the CHF obtained is only around 0.4% of the maximum heat flux that can conceivably be achieved in a phase transition process. In fact, according to Gambill and Lienhard, 'if one could contrive to collect every vapour molecule that leaves a liquid–vapour interface without permitting any vapour molecules to return to the liquid,' the highest heat flux attainable can be estimated by:

$$q''_{max} = \rho_g \lambda \sqrt{\left(\frac{RT}{2\pi}\right)} \tag{3}$$

where R is the ideal gas constant on a unit mass basis. Under the conditions that allowed a CHF of 30 MW m^{-2} to be reached, equation (3) provides a maximum

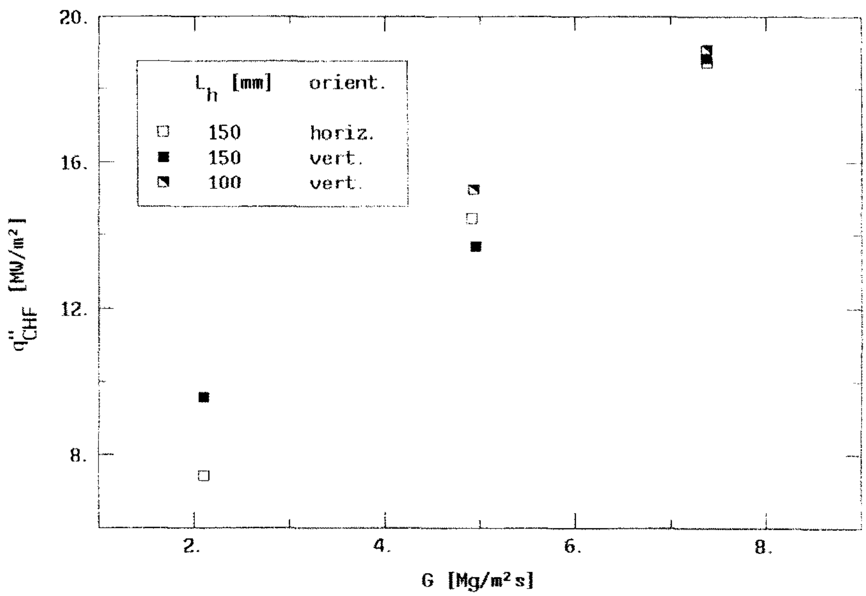

FIG. 8. Influence of the heated length and of the orientation of the test channel on the CHF.

theoretical heat flux of about 7000 MW m^{-2}. According to Gambill and Lienhard, the most serious restriction that prevents reaching this limit in practice 'is that many vapour molecules will inevitably be returned to the interface by molecular collisions'. The return flow of vapour molecules can only be slowed, not eliminated. 'Another problem lies in the premise that all the heat ultimately passes through a liquid–vapour interface. The problem is to get the heat to flow through the liquid, up to an interface, and away from the interface on the vapour side.' We contrived to do this with the help of turbulent promoters, or swirl inserts, such as helically coiled wires.

As already described in this report, helically coiled wires were used in the past [11–14] as turbulence promoters to enhance the heat transfer in single-phase flow (air, water, water–glycerol solution, oil) both in laminar and in turbulent flow. Enhancement of heat transfer was found (and expected) to be coupled with much larger increase in frictional power loss. Anyway no application to the enhancement of CHF in highly subcooled flow boiling was found in literature. We used helically coiled wires of spring steel, fixed (welded) at the inner ends of the heated channel (at the height of the copper clamps). Their task was to increase eddy diffusive heat transfer and continuously remove the thermal boundary layer to prevent and/or delay bubble formation/growth, giving rise to an increase of the overall effectiveness of the coolant. Results are shown in Fig. 9, where the ratio between the CHF with the wire and the CHF without wire inside the tube is plotted vs mass flux (top figure), and the ratio of the relative pressure drops is plotted always vs mass flux (bottom figure). Data are grouped according to the geometric characteristics of the wires. Unless differently specified, data refer to 3.5 MPa, while data at 5.0 MPa refer to a wire diameter of 1.0 mm. The maximum increase of the CHF is up to a factor of about 1.5 for liquid velocities higher than 7.0 m s^{-1} obtained with 1.0 mm diameter wire. Wires with smaller diameters would seem to be less effective on the CHF enhancement, perhaps because of a less mechanical stiffness to the force exerted by the fluid flow at these high velocities. Low velocity tests reveal very scattered and, as an average, a low efficiency in CHF enhancement. This is probably due to the fact that the relative roughness (wire diameter/hydraulic diameter of the channel) of the turbulence promoters determines the Reynolds number, and then the velocity, at which the promoters become effective, as stated by Sutherland [11], who established the heat transfer performance of boundary-layer turbulence promoters. The most efficient wire diameter for CHF enhancement is observed to be 1.0 mm, while the effect of relative spacing of promoters (pitch) can be considered negligible in the range 5–20 mm for the same wire. Sutherland observed a similar behaviour in the heat transfer performance. None the less, pressure drop is inversely related to the wire pitch, as a pitch of 20.0 mm gives rise to an increase of the pressure drop (with respect to the smooth channel) of about 25% (1.0 mm wire diameter), while a pitch of 5.0 mm causes an increase of about 100%.

The effect of the pressure on the heat transfer performance (CHF enhancement) is observed to be negative, in the sense that tests carried out at 5.0 MPa reduce to only 30% the increase of the CHF produced by the wire. This negative effect of the pressure on the turbulence promoters efficiency was also recently observed by Nariai *et al.* [14] using twisted tapes as

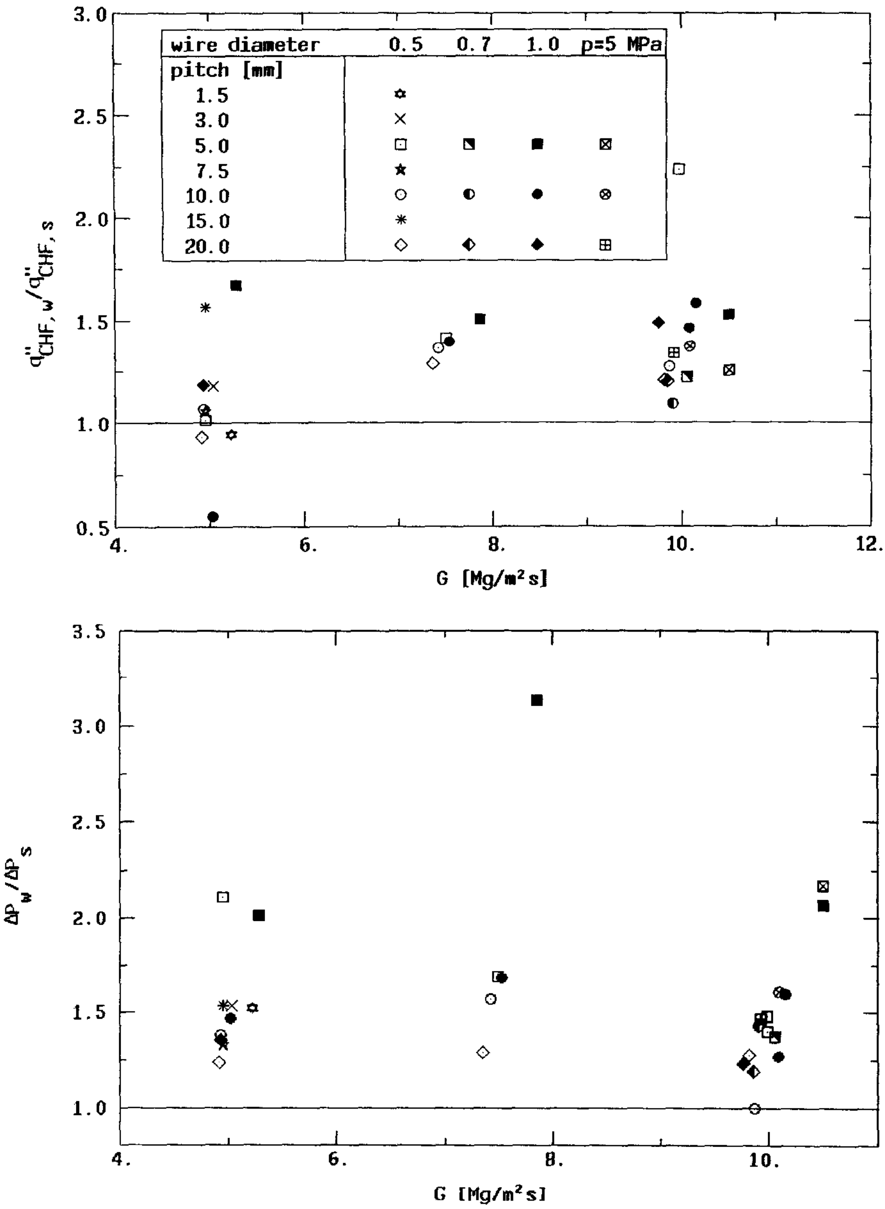

FIG. 9. Influence of the helically coiled wires on the CHF (top figure) and on the pressure drop (bottom figure). If not specified data points refer to 3.5 MPa.

turbulence promoters. In that case authors observed that above 1.0 MPa the CHF enhancement effect of twisted tapes disappeared. Such an experimental observation was also reported experimentally by Gambill *et al.* [16]. As, other conditions being equal, an increase of the pressure produces an increase of the subcooling (and therefore of the CHF), in absolute terms it is possible to have (as indeed we have in the present experiment) the highest CHF at the highest pressure ($p = 5.0$ MPa). Speaking in relative terms, we only observed a reduction in the efficiency of the turbulence promoter, i.e. maximum heat flux enhancement obtained with reference to the smooth channel, with increasing the pressure.

It is interesting to observe instead, that, contrary to the performance of twisted tapes (e.g. [15, 16]), where the increase of the thermal efficiency and the associated increase of the pressure drop are strictly interrelated, in the case of helically coiled wires the thermal efficiency is practically independent of the pressure drop. This latter can be properly reduced decreasing relative spacing of promoters, without affecting the thermal performance of the turbulence promoter.

ENGINEERING PERFORMANCE OF HEAT TRANSFER TECHNIQUES

As we observed, it is possible to increase the CHF in subcooled flow boiling even though it is often

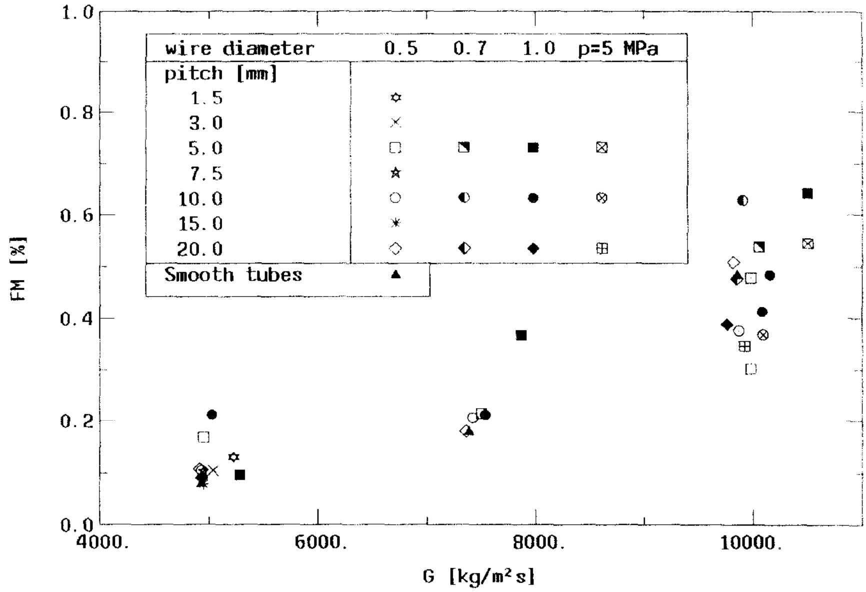

FIG. 10. Evaluation of the figure of merit, *FM*, vs mass flux for all the tests.

necessary to pay a corresponding increase of the pumping power (high velocity in smooth tubes, presence of wires, etc.). Once the heat flux to be removed has been established, engineering performances of different techniques may be achieved comparing them with the figure of merit, *FM*, defined as follows:

$$FM = \frac{\text{pumping power}}{(\text{exchanged thermal power})_{\text{CHF}}} \times 100. \qquad (4)$$

Among different CHF enhancement techniques capable of removing the same heat flux, that presenting the lowest *FM* has to be preferred from the hydraulic viewpoint. The technique can be considered adequate from an engineering viewpoint if *FM* is less than 1%. Figure 10 shows the calculated *FM* values for all tests. The figure of merit is, as expected, an increasing function of mass flux. Helically coiled wire tests present in all cases *FM* values lower than 0.8%, showing more or less the same order of magnitude as smooth tube tests. The test performed with a 1.0 mm wire, 20.0 pitch, that gives rise to an increase of the CHF of 50% with a 25% increase of pressure drop, has an *FM* less than 0.4%. This is a further confirmation of the goodness of coiled wires as turbulence promoters to be used for the enhancement of CHF in subcooled flow boiling at high liquid velocity.

PREDICTION OF CHF EXPERIMENTAL DATA

Prediction of CHF experimental data in smooth tube tests has been tackled using correlations and models available in the literature.

Correlations

Scarcity of data in the range of interest implies also a lack of suitable correlations for the prediction of subcooled CHF. The only possibility is to make use of available correlations, recommended for ranges of validity completely different from those of interest, evaluating the possibility to use them with a certain reliability outside the proposed ranges. Among the many correlations available in the literature, reviewed in ref. [5] and tested in ref. [6], we report here those correlations that are able to provide a consistent prediction of present data.

- Westinghouse [17]:

$$\begin{aligned} q''_{\text{CHF}} &= (0.23\times 10^{6}+0.094G)(3+0.01\Delta T_{\text{sub}}) \\ &\quad \times [0.435+1.23\exp(-0.0093L/D)]^{*} \\ &\quad \times \left\{1.7-1.4\exp\left[-0.532 \right.\right. \\ &\quad \left.\left. \times \left(\frac{h_{\text{sat}}-h_{\text{in}}}{\lambda}\right)^{3/4}\left(\frac{\rho_{\text{g}}}{\rho_{\text{f}}}\right)^{1/3}\right]\right\} \end{aligned} \qquad (5)$$

recommended in the ranges: $0.3 < G < 11$ Mg m^{-2} s^{-1}; $5.7 < p < 20.0$ MPa; $1.25 < q''_{\text{CHF}} < 12.5$ MW m^{-2}; $0 < \Delta T_{\text{sub}} < 126$ K.

- Levy [18]

$$q''_{\text{CHF}} = q''_{\text{pb}} + q''_{\text{conv}} + F$$

$$q''_{\text{pb}} = 0.131\lambda\rho_{\text{g}}\left[\frac{\sigma g^{2}(\rho_{1}-\rho_{\text{g}})}{\rho_{\text{g}}^{2}}\right]^{1/4}$$

$$q''_{\text{conv}} = 0.696(K\rho_{1}C_{\text{p}})^{1/2}\left(\frac{\rho_{1}-\rho_{\text{g}}}{\sigma}\right)^{1/4}$$

$$\times\left[\frac{\sigma g^2(\rho_l-\rho_g)}{\rho_g^2}\right]^{1/8}\Delta T_{sub}$$

$$F = h_l(T_w - T_{sat}) + h_l \Delta T_{sub}$$

$$T_w - T_{sat} = \frac{60}{e^{p/900}}\left(\frac{q''}{10^6}\right)^{1/4}$$

$$h_l = 0.023\frac{K}{D}Re^{0.8}\,Pr^{1/4} \tag{6}$$

recommended in the ranges: $0.6 < G < 11$ Mg m^{-2} s^{-1}; $0.4 < p < 20.0$ MPa; $2 < D < 12$ mm.

- Tong [19]:

$$\frac{q''_{CHF}}{\lambda} = C\frac{G^{0.4}\mu_f^{0.6}}{D^{0.6}} \tag{7}$$

$$C = 1.76 - 7.433x_{ex} + 12.222x_{ex}^2 \tag{8}$$

where λ is the latent heat and μ_f is the dynamic viscosity of saturated liquid (SI units). Tong correlation may also be presented in the form

$$Bo = \frac{C}{Re^{0.6}} \tag{9}$$

where Bo and Re are the boiling number and Reynolds number, respectively. We modified the parameter C, together with a slight modification of the Reynolds number power, to give a more accurate prediction in the range of pressures below 5.0 MPa, as the Tong correlation was recommended for pressures higher than 7.0 MPa. In addition to the present data, we based the modification also on data with 2.5 mm i.d. tubes [20, 21]. The new expression of the Tong correlation is

$$Bo = \frac{C}{Re^{0.5}} \tag{10}$$

with

$C = (0.216 + 4.74\times10^{-2}p)\Psi$ [p in MPa]
$\Psi = 0.825 + 0.986x_{ex}$ if $x_{ex} > -0.1$;
$\Psi = 1$ if $x_{ex} < -0.1$
$\Psi = 1/(2+30x_{ex})$ if $x_{ex} > 0$ (exit saturated conditions).

Comparison with experimental data is shown in Fig. 11, where the ratio between the experimental data and the calculated values of CHF is plotted vs exit pressure. The above correlations are able to provide predictions of data within $\pm 25\%$. Of course modified-Tong correlation provides the best agreement being partially adjusted on the present data-set.

Models

As it is known, models have the advantage, with respect to correlations, of being able to characterize not only the existing and developing data base, but also to be used to predict CHF beyond the established data base. In this sense visual information, not available so far in detail, would be of great help for a full understanding of the basic mechanisms of CHF in subcooled flow boiling at high liquid velocity and inlet subcooling, enabling the development of a mechanistic model of CHF more adherent to reality. Anyway, at the moment, three different models are available in literature for the prediction of the CHF in subcooled flow boiling: the Weisman and Ileslamlou [22], the Lee and Mudawar [23] and the Katto [24] models.

The Weisman and Ileslamlou model [22], based on the existence of a bubbly layer adjacent to the heater surface and assuming the turbulent interchange at the outer edge of the bubbly layer as the limiting mechanism, was proposed as an extension of the Weisman and Pei model [25] and assessed within the following parameters ranges: $-0.12 \geqslant x_{ex} \geqslant -0.46$; $p = 6.8$–19 MPa; $D = 1.9$–37.5 mm; $L = 76$–1950 mm; $G = 1.3$–10.5 Mg m^{-2} s^{-1}. The Lee and Mudawar model [23] is a mechanistic CHF model based on the existence of a vapour blanket forming close to the heated wall by the coalescence of small bubbles, and assuming the dryout of the liquid sublayer between the vapour blanket and the heated wall to be triggered by a Helmholtz instability at the sublayer–vapour blanket interface. The model was assessed by the authors (choice of correlations) on the following ranges of parameters: $p = 5$–17.6 MPa; $G = 1$–5.2 Mg m^{-2} s^{-1}; $D = 4$–16 mm; $\Delta T_{sub} = 0$–59 K. The two models reported above were proposed by respective authors for high pressure conditions. In particular, the Lee and Mudawar model was developed for high pressure conditions only since it assumed the existence of a vapour layer in a small wall region while maintaining a velocity profile in the core liquid which can be represented by the law of the wall. This condition is simply not valid for low pressure systems. Similar considerations could be forwarded for the Weisman and Ileslamlou model. Both models are therefore not expected to yield very accurate CHF predictions at low pressures.

The Katto model [24] is based on the same mechanism as the Lee and Mudawar model, from which it borrows much of the original derivation, i.e. liquid sublayer dryout mechanism. A thin vapour layer or slug (called 'vapor blanket') is formed due to accumulation and condensation of the vapour coming from the wall, overlying a very thin liquid sublayer adjacent to the wall. CHF is assumed to occur when the liquid sublayer is extinguished by evaporation during the passage time of the vapour blanket sliding on it. Parameters to be determined in the description of the mechanistic model by Katto are: initial thickness of the sublayer, δ, vapour blanket length, L_B, and velocity, U_B. The evaluation of δ, different from the Lee and Mudawar model, is obtained using a non-dimensional correlation derived in a previous study of CHF in pool boiling [26]. Vapour blanket length L_B is set equal to the critical wavelength of Helmholtz instability of the liquid–vapour interface (same as Lee and Mudawar model). Vapour blanket velocity U_B is

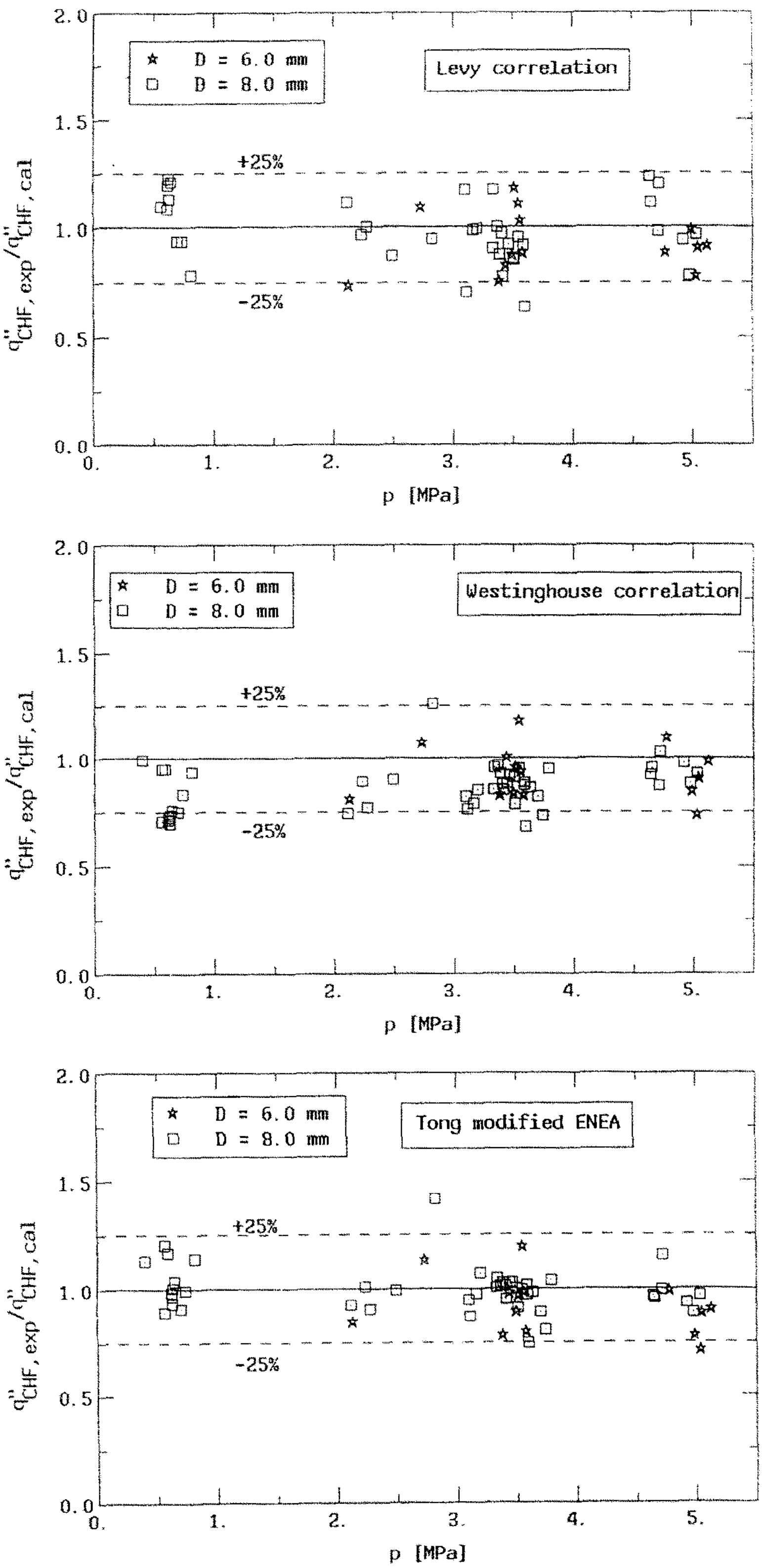

FIG. 11. Comparison between measured and predicted CHF using Westinghouse [17], Levy [18], and modified-Tong [19] correlations.

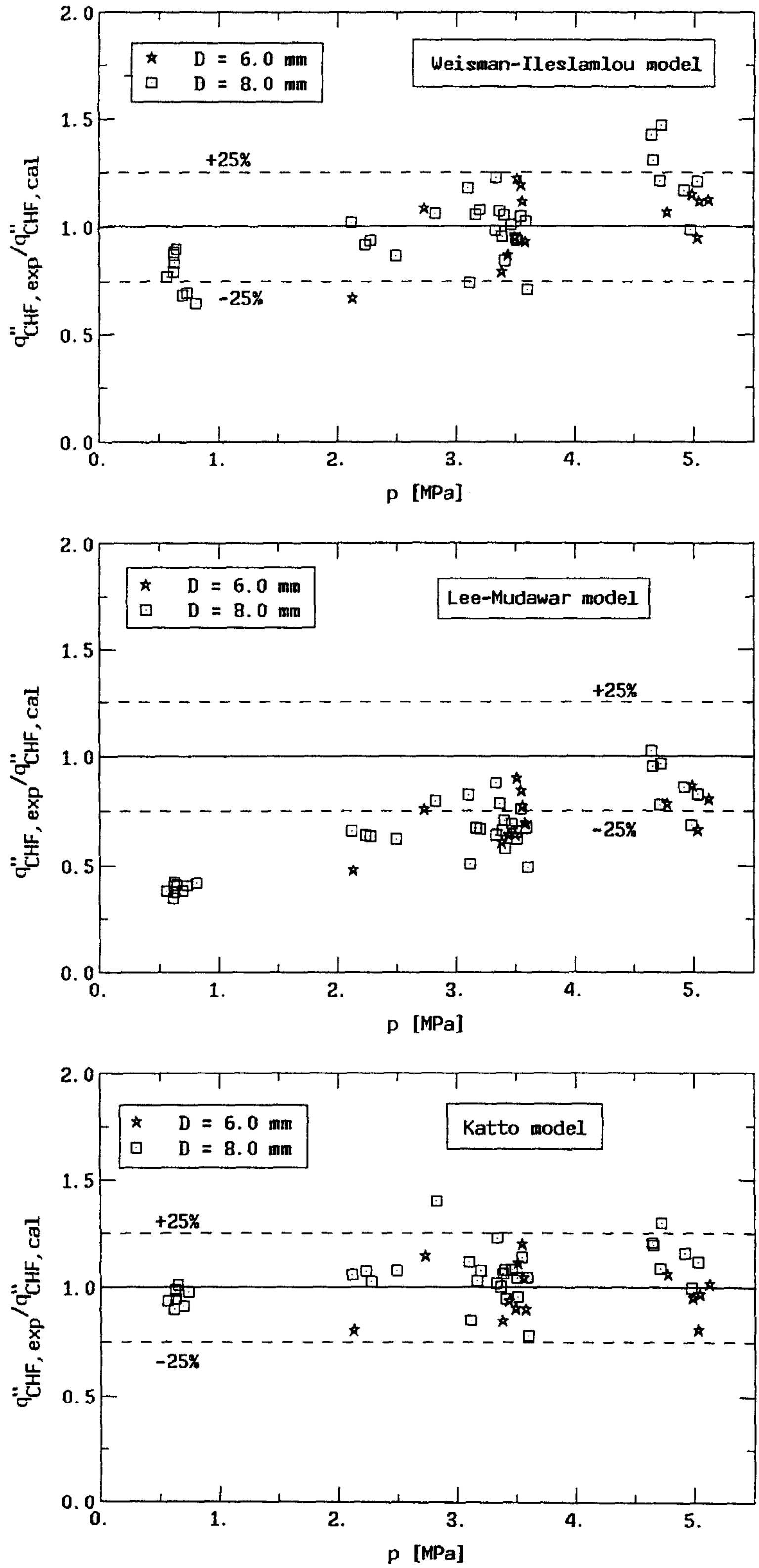

FIG. 12. Comparison between measured and predicted CHF using Weisman–Ileslamlou [22], Lee–Mudawar [23], and Katto [24] models.

evaluated by relating it to the local velocity U_δ of the two-phase flow (which is assumed to be homogeneous flow) at a distance δ from the tube wall. U_δ is evaluated using the Karman velocity distribution and U_B is equal to kU_δ, where k is called velocity coefficient and is the only quantity to be determined empirically in the Katto model. The velocity coefficient k (non-dimensional correlation as a function of Reynolds number, liquid and vapour density, and void fraction) was derived on data-sets published in [20, 21] and [27–30], practically transforming the model in an empirical correlation. The Katto model is assessed on the following range of parameters (water): $D = 1.14$–11.07 mm; $p = 0.1$–19.6 MPa; $G = 0.35$–40.6 Mg m^{-2} s^{-1}; $\Delta T_{sub,out} = 0$–117.5 K.

A comparison of CHF data with predictions provided by the above three models is shown in Fig. 12. The Weisman–Ileslamlou model provides predictions affected by a systematic effect of the pressure, even though, globally, most of predictions would seem to lie within $\pm 25\%$. The Lee–Mudawar model, as expected, gives a general inadequacy for the prediction of present data. Good predictions are provided by the Katto model, that was assessed on a relatively low pressure data set, besides high pressure data. Although mechanistic in nature, the three models presented above show the necessity of empirical parameters introduced in the mathematical description of the dynamics of the bubbles. Also the Katto model, that provides consistent predictions of present data, introduces the velocity coefficient k, that must be derived from experiments. It is therefore still necessary to accomplish a full understanding of the phenomenon to propose a realistic and pure mechanistic model description.

CONCLUSIONS

Principal concluding remarks regarding smooth channel tests are:

- the main thermal hydraulic parameters affecting the CHF are the liquid velocity and the liquid subcooling;
- the direct effect of the pressure on the CHF turned out to be negligible, even though a higher pressure enables us to reach higher inlet subcoolings at the inlet of the channel;
- in the present range of high liquid velocity, negligible effect of the orientation of the channel on the CHF was observed;
- a maximum CHF of about 30 MW m^{-2} was reached with smooth tubes under the following conditions: $T_{in} = 30$ C, $p = 5.0$ MPa, $u = 10$ m s^{-1}, $D = 8.0$ mm, $L = 0.1$ m.

Regarding the use of turbulence promoters for the enhancement of the CHF, the following conclusions may be drawn:

- helically coiled wires ($d = 1.0$ mm, pitch $= 20.0$ mm) allowed an increase of the CHF up to 50%, with reference to smooth channels, coupled with a moderate increase of pressure drop (25%);
- pressure revealed a negative effect on the relative efficiency of turbulence promoters.

Acknowledgements—The research was partially funded by NET, Next European Torus (25%) and by the Fusion Department of ENEA, NUC-FUS (75%). The authors wish to thank Mrs A. M. Moroni for her help in the editing of the paper.

REFERENCES

1. A. E. Bergles, J. G. Collier, J. M. Delhaye, G. F. Hewitt and F. Mayinger, *Two-Phase Flow and Heat Transfer in the Power and Process Industries*, pp. 226–255. Hemisphere, New York (1981).
2. J. G. Collier, *Convective Boiling and Condensation*, pp. 144–177. McGraw-Hill, New York (1981).
3. Y. Y. Hsu and R. W. Graham, *Transport Processes in Boiling and Two-Phase Systems*, pp. 217–232. American Nuclear Society (1986).
4. R. D. Boyd, Subcooled flow boiling Critical Heat Flux (CHF) and its application to fusion energy components. Part I: a review of fundamentals of CHF and related data base, *Fusion Technol.* **7**, 7–30 (1985).
5. R. D. Boyd, Subcooled flow boiling Critical Heat Flux (CHF) and its application to fusion energy components. Part II: a review of microconvective, experimental, and correlational aspects, *Fusion Technol.* **7**, 31–52 (1985).
6. G. P. Celata, A review of recent experiments and predictions aspects of burnout at very high heat flux, *Proceedings of the International Conference on Multiphase Flows '91—Tsukuba*, Vol. 3, pp. 31–40 (1991).
7. M. Cumo, G. E. Farello and G. C. Pinchera, Determinazioni sperimentali della lunghezza di assetto fluidodinamico in canali a sezione circolare, *Proceedings of the 20th National Conference ATI*, Vol. 1, pp. 70–79 (1965) (in Italian).
8. F. C. Gunther, Photographic study of surface-boiling heat transfer to water with forced convection, *Trans. ASME* **73-2**, 115–123 (1951).
9. G. P. Celata, M. Cumo, F. Inasaka, A. Mariani and H. Nariai, Influence of channel diameter on subcooled flow boiling burnout at high heat fluxes, *Int. J. Heat Mass Transfer* **36**, 3407–3410 (1993).
10. W. R. Gambill and J. H. Lienhard, An upper bound for the critical boiling heat flux, *J. Heat Transfer* **111**, 815–818 (1989).
11. W. A. Sutherland, Improved heat-transfer performance with boundary-layer turbulence promoters, *Int. J. Heat Mass Transfer* **10**, 1589–1599 (1967).
12. P. Kumar and R. L. Judd, Heat transfer with coiled wire turbulence promoters, *Can. J. Chem. Engng* **48**, 378–383 (1970).
13. R. Sethumadhavan and M. Raja Rao, Turbulent flow heat transfer and fluid friction in helical-wire-coil-inserted tubes, *Int. J. Heat Mass Transfer* **26**, 1833–1845 (1983).
14. S. B. Uttarwar and M. Raja Rao, Augmentation of laminar flow heat transfer in tubes by means of wire coil insert, *J. Heat Transfer* **107**, 930–935 (1985).
15. H. Nariai, F. Inasaka, W. Fujisaki and H. Ishiguro, Critical Heat Flux of subcooled flow boiling in tubes with internal twisted tapes, *Proceedings of the ANS Winter Meeting, Session on Fundamentals of Fusion Reactors Thermal-Hydraulics THD*, Vol. 1, pp. 38–46 (1991).
16. W. R. Gambill, R. D. Bundy and R. W. Wansbrough, Heat transfer, burnout and pressure drop for water in

swirl flow through tubes with internal twisted tapes, *Chem. Engng Prog. Symp. Ser.*, n. 32, Vol. 52, p. 127 (1961).
17. L. S. Tong, H. B. Currin and A. G. Thorp, An evaluation of the departure from nucleate boiling in bundles of reactor fuel rods, *Nucl. Sci. Engng* **33,** 7–15 (1968).
18. S. Levy, Prediction of the Critical Heat Flux in forced convection flow, General Electric Report GEAP—3961 (1962).
19. L. S. Tong, Boundary-layer analysis of the flow boiling crisis, *Int. J. Heat Mass Transfer* **11,** 1208–1211 (1968).
20. G. P. Celata, M. Cumo and A. Mariani, Subcooled water flow boiling CHF with very high heat fluxes, *Revue Générale de Thermique* **362,** 106–114 (1991).
21. G. P. Celata, M. Cumo and A. Mariani, Burnout in highly subcooled flow boiling in small diameter tubes, *Int. J. Heat Mass Transfer* **36,** 1269–1285 (1993).
22. J. Weisman and S. Ileslamlou, A phenomenological model for prediction of Critical Heat Flux under highly subcooled conditions, *Fusion Technol.* **13,** 654–659 (1988). (Corrigendum in *Fusion Technol.* **15,** 1463 (1989).)
23. C. H. Lee and I. Mudawar, A mechanistic Critical Heat Flux model for subcooled flow boiling based on local bulk flow conditions, *Int. J. Multiphase Flow* **14,** 711–728 (1988).
24. Y. Katto, A prediction model of subcooled water flow boiling CHF for pressure in the range 0.1–20.0 MPa, *Int. J. Heat Mass Transfer* **35,** 1115–1123 (1992).
25. J. Weisman and B. S. Pei, Prediction of the Critical Heat Flux in flow boiling at intermediate qualities, *Int. J. Heat Mass Transfer* **26,** 1463–1477 (1983).
26. Y. Haramura and Y. Katto, A new hydrodynamic model of Critical Heat Flux, applicable widely to both pool and forced convection boiling on submerged bodies in saturated liquids, *Int. J. Heat Mass Transfer* **26,** 389–399 (1983).
27. R. D. Boyd, Subcooled water flow boiling transition and the L/D effect on CHF for a horizontal uniformly heated tube, *Fusion Technol.* **18,** 317–324 (1990).
28. F. Inasaka and H. Nariai, Critical Heat Flux of subcooled flow boiling with water, *Proceedings of the NURETH-4*, Vol. 1, pp. 115–120 (1989).
29. Heat Mass Transfer Section, Scientific Council, Academy of Sciences, U.S.S.R., Tabular data for calculating burnout when boiling water in uniformly heated round tubes, *Thermal Engng* **23,** 77–79 (1972).
30. B. Thompson and R. V. Macbeth, Boiling water heat transfer burnout in uniformly heated round tubes: A compilation of world data with accurate correlations, U.K.A.E.A., AEEW-R 359 (1964).